AKADÉMIAI KIADÓ

Optimization by RSM on rotary friction welding of AA1100 aluminum alloy and mild steel

F. KHALFALLAH[1,2*], Z. BOUMERZOUG[1], S. RAJAKUMAR[3] and E. RAOUACHE[4]

[1] Department of Mechanical Engineering, University of Biskra, B.P. 145, Biskra, Algeria

[2] Department of Physics, Faculty of Science, University of M'sila, M'sila, 28000, Algeria

[3] Centre for Materials Joining & Research, Department of Manufacturing Engineering, Annamalai University, India

[4] Civil Engineering Department, University of Bordj Bou Arreridj, Algeria

International Review of Applied Sciences and Engineering

11 (2020) 1, 34-42

DOI:
10.1556/1848.2020.00005

Received: January 31, 2019 • Accepted: March 20, 2019
Published online: April 18, 2020

ORIGINAL RESEARCH PAPER

ABSTRACT

The objective of this work is to investigate the rotary friction welding of AA1100 aluminum alloy with mild steel, and to optimize the welding parameters of these dissimilar materials, such as friction pressure/time, forging pressure/time and rotational speed. The optimization of the welding parameters was deduced by applying Response Surface Methodology (RSM). An empirical relationship was also applied to predict the welding parameters. Tensile test and micro-hardness measurements were used to determine the mechanical properties of the welded joints. Some joints were analyzed by scanning electron microscopy (SEM) and energy dispersive X-ray spectroscopy (EDS) in order to investigate the formation of intermetallic compound (IMC) layer at the weld interface. Experimentally, the tensile strength of the weld increases with increasing the forging pressure/time, while the low level of forging pressure/time allows the formation of an IMC layer which reduces the tensile strength of the weld.

KEYWORDS

optimization, response surface methodology, rotary friction welding, AA1100 aluminum alloy, mild steel

1. INTRODUCTION

Today, the joining of aluminum alloys with steel is widely used in the automotive industry, since reducing the weight of vehicles is one of the effective measures to save energy and preserve the environment. The interest to this combination of materials is mainly due to the light weight, high heat conductivity and corrosion resistance characteristics of aluminum alloys that compliment well with the high strength and toughness of steel [1].

In general, the joints of metals are made by welding processes. In welding of aluminum alloys to steel, the formation of an intermetallic compound (IMC) is necessary to achieve an effective bond between the two metals. However, in the case of fusion welding steel/aluminum, the excessive formation of IMC, in particular, the Al-rich phases, degrades the joint strength [2]. To avoid the formation of such brittle IMC, some technical conditions should be satisfied, i.e., welding should occur in the solid state at low temperature and in short time [3]. The friction welding (FW) is a solid state welding process; it is one of the most suitable methods for joining aluminum alloys to steel [4]. Rotary Friction Welding (RFW) is the most commonly used method in friction welding. It can be applied in two ways: continuous drive friction welding and inertia friction welding [5]. However, the RFW process has a limitation of use, since it cannot be used for welding parts with a non-circular cross-section [6].

*Corresponding author. Department of Mechanical Engineering, University of Biskra, B.P. 145, Biskra, Algeria
E-mail: fa_fares@yahoo.fr, fares.khalfallah@univ-msila.dz.

In continuous drive method, a rotating sample is pressed against a stationary sample as shown in Fig. 1(a and b). The friction at the interface generates the welding heat, which upset the samples (Fig. 1c). Finally, the rotation stops and a forging pressure is introduced to achieve the bonding (Fig. 1d) [7, 8].

As it is reported, several welding parameters affect the quality of friction welds, such as friction time, forging time, friction pressure, forging pressure, and rotational speed [9, 10]. Figure 2 shows the parameters and the phases of continuous drive friction welding. In general, RFW consists of two phases: a friction phase to generate the necessary heat and a forging phase to consolidate the weld [11].

According to the literature, some researchers had investigated the friction welding of aluminum alloys with steel [12–16]. Fukumoto et al. [13, 14] carried out a rotary friction welding of AISI 304 austenitic-stainless steel with aluminum and proved that the friction welding process was very efficient in the welding of these dissimilar materials. They reported that strength increase as the friction time increase, but a longer friction time caused the excess formation of Fe–Al based IMC layer at the friction weld interface, which decreases the strength of joint. Sahin [17] studied also the rotary friction welding of AISI 304 austenitic-stainless steel with aluminum. He has shown that friction time, friction pressure, and forging pressure have a strong effect on tensile strength, microstructures, and hardness of joints.

In addition, Alves et al. [18] studied the rotary friction welding of AA 1050 aluminum alloy to AISI 304 austenitic-stainless steel and showed that the strength of the joints varied with friction time and other welding parameters. Meshram et al. [19] developed a rotary friction welding of AISI 4340 austenitic-stainless steel with AA6061 aluminum alloy, using a silver interlayer as a diffusion barrier for Fe. They found that silver interlayer avoids the formation of the brittle IMC layer, and increases the tensile strength of welds.

However, Wan et al. [20] investigated the effects of friction time on microstructure characteristics and mechanical properties of friction welding AISI 316L steel to AA6061 aluminum alloy. They machined a welding groove of 15° on the end of steel part to help control the growth of IMC layers. The thickness of IMC layers increased with elevated friction time, while the machining of the welding groove reduced the IMC layer thickness. The tensile strength reached 166.32 MPa in the case of the welding groove; it was higher than that of the joint without welding groove [20].

In addition to the experimental investigation, new statistical methods were applied to determine the optimum parameters, i.e., to reduce the number of the experiments [21–23]. In this approach, Paventhan et al. [21] used Response Surface Methodology (RSM) as a statistical approach to optimize the welding parameters for achieving an optimum tensile strength of AA6082 alloy to AISI 304 austenitic stainless steel joints. Pachal et al. [22] used Taguchi Experiment Design Technique to optimize welding parameters for maximizing tensile strength of friction welding AA 6061 Al alloy to AISI 304. Mathiazhagan et al. [23] developed an empirical relationship between the welding parameters and the tensile property of the welded AA 6063 Al alloy and AISI 304, using the RSM technique and the Adaptive Neuro-Fuzzy Inference System (ANFIS) technique.

In this study, an attempt was made to optimize friction welding parameters for achieving optimum mechanical properties such as tensile strength and hardness of welded AA1100 aluminum alloy to mild steel, using the Response Surface Methodology (RSM) and statistical software as Design Expert. In addition, some joints were characterized by scanning electron microscopy (SEM) and energy dispersive X-ray spectroscopy (EDS).

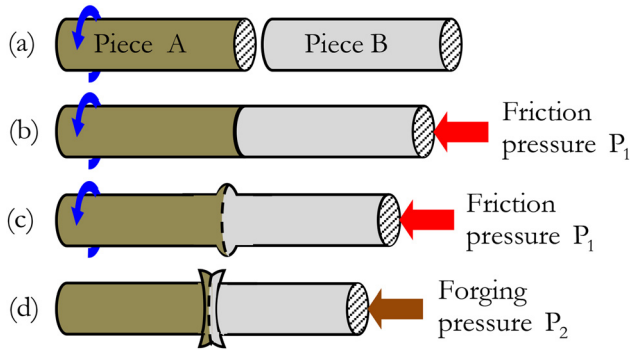

Figure 1. Rotary friction welding process

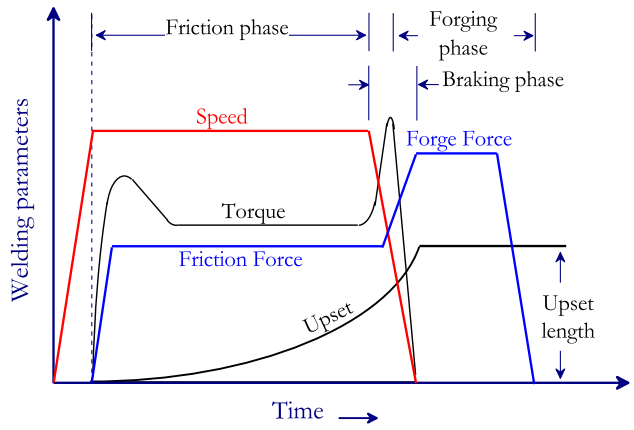

Figure 2. Parameters and phases of continuous drive friction welding [6]

2. EXPERIMENTAL PROCEDURE

2.1. Welding process

The materials used in this experimental work were aluminum AA1100 and mild steel. They were cylindrical rods with 12 mm in diameter and 70 mm in length, as shown in Fig. 3. Table 1 presents the chemical compositions of these two dissimilar materials determined by X-ray fluorescence (XRF) technique.

Figure 3. Macrographic view of AA1100 aluminum alloy and mild steel specimens before welding

The welding process was carried out using a continuous drive friction welding machine (Rexroth, R.V. Machine tools) as shown in Fig. 4. The rotating workpiece is the mild steel rod, while the non-rotating work piece is the aluminum rod. Before the welding process, the ends of samples were polished and cleaned to reduce the effect of contaminants, especially grease, which can affect the quality of joints.

2.2. Response surface methodology (RSM)

The effect of friction welding parameters on the properties of the joints can be carried out using the Response Surface Methodology (RSM). RSM is a design of experiment (DOE) technique which is used for prediction or optimization. It is a statistical approach employed for analyzing and developing the effect of different independent variables (named the factors x_i) on a dependent variable (response). The objective is to optimize this response [24, 25]. The advantage of using RSM or other DOE techniques is to reduce the number of experiments.

In this study, the optimization of welding parameters that influence the tensile strength (TS) and micro-hardness (MH), was performed by RSM technique, based on selecting three-factors and five-levels factorial design matrix. The three welding parameters selected in this work are:

- Friction pressure/time $= \frac{\text{Friction pressure}}{\text{Friction time}}$;
- Forging pressure/time $= \frac{\text{Forging pressure}}{\text{Forging time}}$;
- Rotational speed.

The five chosen values for each process parameter are listed in Table 2. The upper and lower levels were coded as +2 and −2, respectively, and the coded value for each level can be calculated from the following relationship:

$$X_i = 2\dot{s}\frac{[2X - (X_{\max} + X_{\min})]}{(X_{\max} - X_{\min})} \quad (1)$$

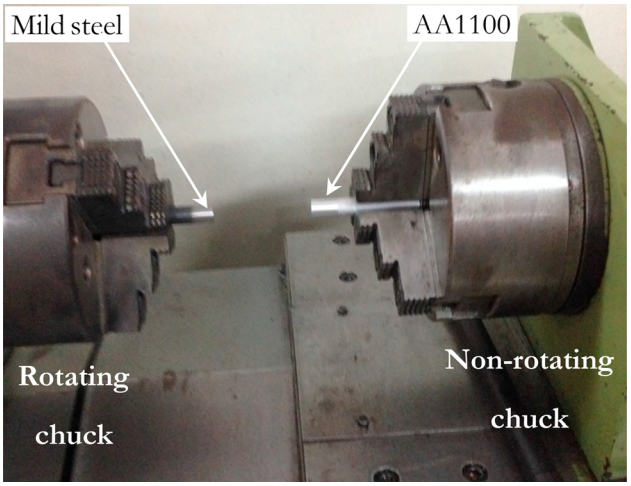

Figure 4. General view of a part of the RFW machine

where X_i is the required coded value of a variable and X is any value of the variable from the lowest level $X_{\min}$ to the highest level $X_{\max}$ [21, 26].

The welding experiments were performed using the parameters dictated by the design matrix presented in Table 3.

The welded samples (Fig. 5a), three for each experiment, were machined and prepared for mechanical and microstructural testing. For the tensile test, the welded specimens are prepared according to ASTM standards (Fig. 5b). After that, they were tested using a 100 kN, servo controlled universal testing machine (Make: FIE–Bluestar, Model: UNITEK 94100) with a crosshead speed of 0.5 mm/min.

For micro-hardness measurements and microstructural analysis, the welded specimens were sectioned, polished, and etched with Keller and Nital reagents. The micro-hardness measurements were recorded using a micro-hardness tester (Make: Shimadzu, Model: HMV-2T) at 200 g load at three different locations in the welded joint. The microstructure of some samples was observed using a scanning electron microscopy (SEM) (Make: JEOL, Model: JSM-6610LV) coupled with energy dispersive X-ray spectroscopy (EDS).

2.3. Developing of empirical relationship

By applying RSM, an empirical relationship between the welding parameters and output response can be established, and used for reach an optimum response value.

Generally, for our study, a second-order polynomial equation is used in the form:

$$y = b_0 + \sum_{i=1}^{n} b_i X_i + \sum_{i=1}^{n} b_{ii} X_i^2 + \sum\sum_{i<j} b_{ij} X_i X_j + \varepsilon \quad (2)$$

Table 1. The chemical composition of aluminum and steel rods (wt%)

Materials	C	Si	S	P	Mn	Cu	Mg	Zn	Fe	Al
AA 1100	–	0.57	–	0.04	–	0.01	0.53	0.02	0.23	98.6
Mild Steel	0.39	0.28	0.03	0.03	0.9	0.14	–	–	98.2	0.03

Table 2. Friction welding parameters and their levels for the central composite design (CCD)

Parameter	Notation	Unit	Level				
			−1.414	−1	0	+1	+1.414
Friction pressure/time	A	MPa/s	3.62	4.08	5.20	6.31	6.77
Forging pressure/time	B	MPa/s	16.79	21.54	33.01	44.47	49.22
Rotational speed	C	rpm	900	930	1,000	1,070	1,100

Table 3. Designed matrix and experimental results

Expt. no.	Coded Values			Actual values			Results	
	A	B	C	A	B	C	TS (MPa)	MH (Hv)
1	+1	+1	−1	6.31	44.47	930	167.44	290.5
2	+1	−1	+1	6.31	21.54	1,070	151.26	299
3	−1	+1	+1	4.08	44.47	1,070	161.56	346.33
4	−1	−1	−1	4.08	21.54	930	161.03	310.67
5	−1.414	0	0	3.62	33.01	1,000	156.01	350.5
6	+1.414	0	0	6.77	33.01	1,000	171.67	266.5
7	0	−1.414	0	5.20	16.79	1,000	156.01	253.5
8	0	+1.414	0	5.20	49.22	1,000	178.46	324
9	0	0	−1.414	5.20	33.01	900	167.29	332
10	0	0	+1.414	5.20	33.01	1,100	152.62	286
11	0	0	0	5.20	33.01	1,000	174.13	288.67
12	0	0	0	5.20	33.01	1,000	174.13	288.67
13	0	0	0	5.20	33.01	1,000	174.13	288.67
14	0	0	0	5.20	33.01	1,000	174.13	288.67
15	0	0	0	5.20	33.01	1,000	174.13	288.67

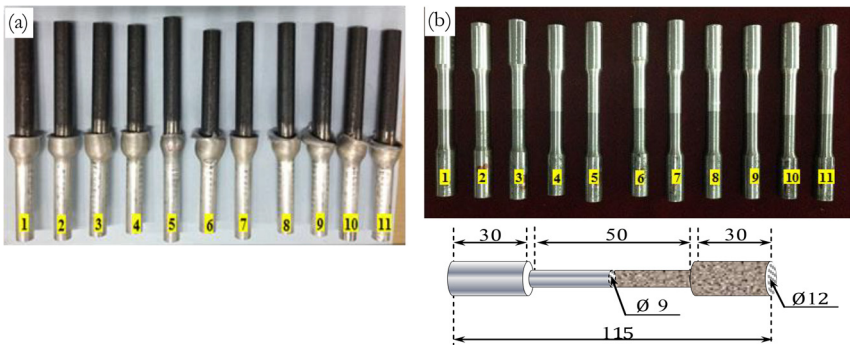

Figure 5. Friction welded samples: (a) Macrographic view ; (b) Tensile testing specimen details (Unit: mm)

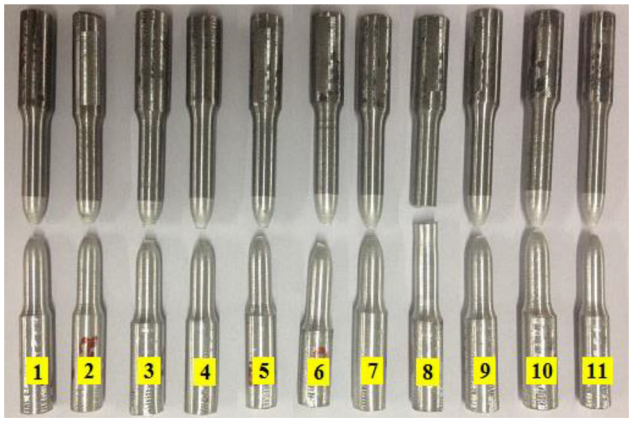

Figure 6. Photograph of samples after tensile test

where, ε represents the noise (error) observed in the response $\boldsymbol{y}$ and n is the factor's number.

In our case, with the use of three factors A, B and C, the selected polynomial could be expressed by:

$$y = b_0 + b_1A + b_2B + b_3C + b_{12}AB + b_{13}AC + b_{23}BC + b_{11}A^2b_{22}B^2 + b_{33}\dot{s}C^2 \quad (3)$$

with b_0 is the average value (intercept) of the response and b_1, b_2, b_3, ... and b_{33} are the regression coefficients [27, 28].

The average value and the other regression coefficients were obtained using small central composite design (CCD) technique, with statistical software as Design Expert 7.0.

3. RESULTS AND DISCUSSION

3.1. Tensile strength testing

The results of the tensile test are shown in Table 3. The maximum value, 178.46 MPa, was recorded in sample 8, which is prepared at the maximum value of forging pressure/time of (49.22 MPa/s). Figure 6 shows the specimens after testing. It can be observed that sample 8 shows a brittle rupture while the others show a ductile rupture (necking shape) [29].

3.2. RSM results

3.2.1. Significance test of the model. To verify the adequacy of the developed model, an analysis of variance (ANOVA) was performed, and the probability of significance of each coefficient was expressed by "Prob > F."

For our investigation, if the "Prob > F" values are less than 0.05, this means that the model terms are significant (the confidence level is 95%) [28].

The ANOVA for the tensile strength (TS) and micro-hardness (MH) is given in Table 4. From this table, it can be understood that the developed relationships are adequate for predicting the tensile strength and hardness of friction welded AA1100 Aluminum alloy–Mild steel at 95% confidence level.

Figure 7 indicates a high degree of correlation between predicted and experimental values for each response, which means that the above model is adequate.

According to the developed model, the empirical relationships for predicting tensile strength and hardness were expressed as follows:

Table 4. Design-expert ANOVA

Source	Sum of Squares	*df*	Mean square	F-value	*P*-value Prob > F	
For TS:						
Model	1155.67	9	128.41	123.60	<0.0001	significant
A	122.62	1	122.62	118.03	0.0001	
B	252.00	1	252.00	242.57	<0.0001	
C	107.60	1	107.60	103.58	0.0002	
Residual	5.19	5	1.04			
Lack of fit	5.19	1	5.19			
Pure error	0	4	0			
Std. deviation	1.02		R^2	0.9955		
Mean	166.27		Adj. R^2	0.9875		
CV (%)	0.61		Pred. R^2	0.5162		
Press	561.58		Adeq. precision	34.350		
For MH:						
Model	10611.89	9	1179.10	495.13	<0.0001	significant
A	3528.00	1	3528.00	1481.48	<0.0001	
B	2485.13	1	2485.13	1043.56	<0.0001	
C	1058.00	1	1058.00	444.28	<0.0001	
Residual	11.91	5	2.38			
Lack of fit	11.91	1	11.91			
Pure error	0	4	0			
Std. deviation	1.54		R^2	0.9989		
Mean	300.16		Adj. R^2	0.9969		
CV (%)	0.51		Pred. R^2	0.8788		
Press	1287.28		Adeq. precision	76.984		

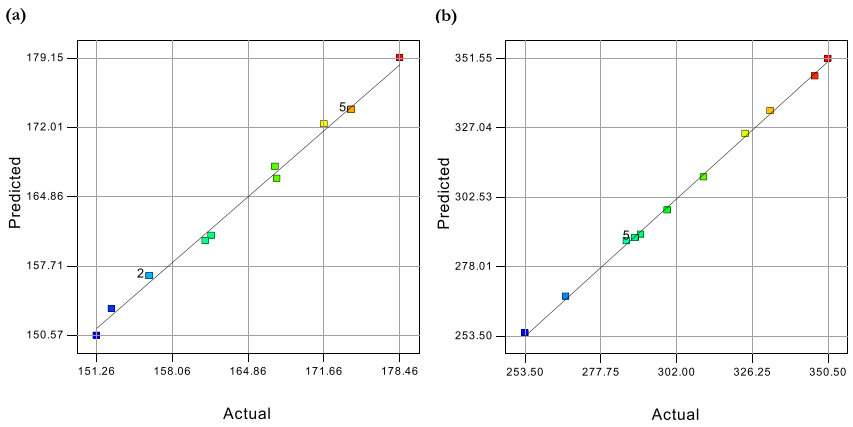

Figure 7. Correlation graph for the response: (a) Tensile strength (TS), (b) Micro-hardness (MH)

Tensile strength:

$$TS = -751.91 - 0.45A - 5.33B + 2.05C - 0.1AB + 0.05AC + 8.03\times10^{-3}BC - 3.76A^2 - 0.02B^2 - 1.32\times10^{-3}C^2 \quad (4)$$

Micro-hardness:

$$MH = 3310.9 - 275.6A + 28.71B - 5.26C - 2.14AB + 0.23AC - 0.02BC + 8.59A^2 + 5.89\times10^{-3}B^2 + 2.18\times10^{-3}C^2 \quad (5)$$

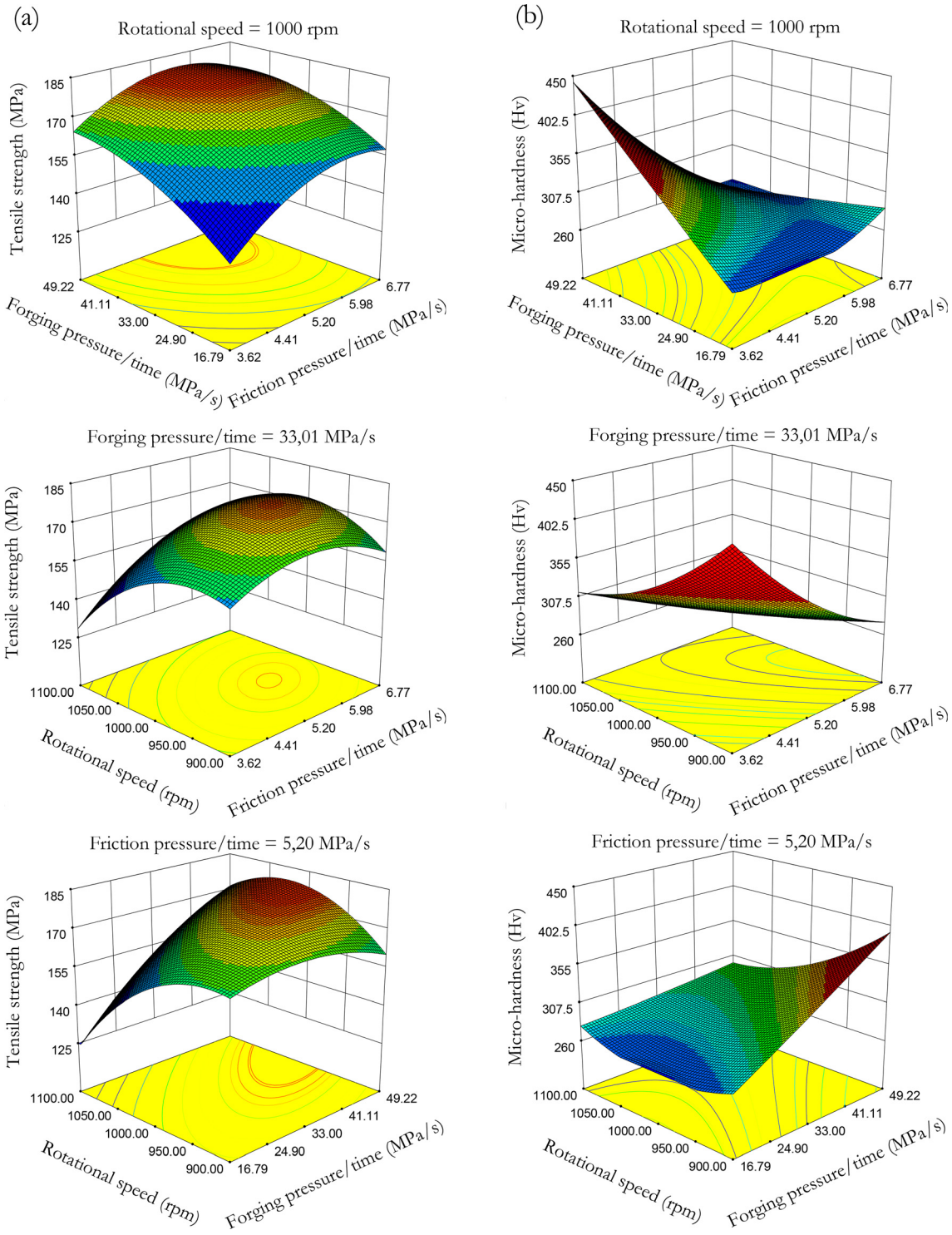

Figure 8. Response plots of welding parameters on: (a) tensile strength (TS); (b) Micro-hardness (MH)

3.2.2. Effect of welding parameters on the responses

Effect of welding parameters on tensile strength (TS). The surface plots in Fig. 8a shows the interaction effect of each two input parameters on the response TS, while the third parameter is on its average level. The tensile strength of the welded joints increased with the increase of forging pressure/time and friction pressure/time, while the increase in rotational speed causes a decrease in tensile strength. By analyzing the response plots, the highest tensile strength value is 178.46 MPa, recorded from sample 8 which is prepared by forging pressure/time at the maximum level of 49.22 MPa/s.

The contribution rank of each welding parameters on tensile strength can be determined from their respective "F-Value" (Table 4), as the degrees of freedom are the same for all the input parameters [21, 30]. The higher *F* value implies that the respective parameter has more influence. From Table 4, it can be concluded that forging pressure/time contributes more to tensile strength and followed by friction pressure/time than the rotational speed.

Effect of welding parameters on micro-hardness (MH). The surface plots of response MH of joints is illustrated in Fig. 8b. The hardness of the welded joints decreased with increasing friction pressure/time and rotational speed. But the increase of forging pressure/time causes an increase in the hardness. The minimum hardness value is 253.5 Hv, corresponding to sample 7, which is prepared at forging pressure/time minimum. From Table 4, the contribution rank of welding parameters is friction pressure/time followed by forging pressure/time than the rotational speed.

Table 5. Optimization criteria used in this study

Parameter and responses	Notation	Criterion	Limit	
			Lower	Upper
Friction pressure/ time (MPa/s)	A	Maximize	3.62	6.77
Forging pressure/ time (MPa/s)	B	Maximize	16.79	49.22
Rotational speed (rpm)	C	In range	900	1,100
Tensile strength (MPa)	TS	Maximize	170	180
Micro-hardness (Hv)	MH	Maximize	250	300

3.2.3. Optimization of welding parameters.

The aim of this part is to find the optimum welding parameters to maximize both the strength and hardness of friction welded joints of AA 1100 to mild steel. The RSM is an ideal method for determination of these optimum welding parameters. The Optimization criteria were set as presented in Table 5, and the optimal solutions were shown in Table 6.

3.2.4. Validation of optimized solutions.

In order to validate the optimized solutions provided by the previous model, three weld experiments were carried out according to the recommended parameters. Table 7 shows the optimum welding parameters, the measured and the predicted values of tensile strength and micro-hardness, and the percentage error. It can be concluded that there is an excellent agreement between measured values and predicted values.

3.3. SEM and EDS analysis

In order to show the effect of the forging pressure/time on the microstructure of the weld interface, SEM observations were performed on samples 7, 11 and 8. These samples are prepared under the same condition of rotational speed (1,000 rpm) and friction pressure/time (5.20 MPa/s), but with different forging pressure/time. Figure 9 displays the SEM images of samples 7, 11 and 8. It is seen from Fig. 9a that a thin layer was formed at the weld interface of sample 7, which was prepared at the low value of forging pressure/time (16.79 MPa/s). The thickness of this layer is ~900 nm. However, a very thin layer or no layer was formed at the weld interface of sample 11 (for an average value of forging pressure/time 33.01 MPa/s) and sample 8 (at maximum

Table 6. Optimal solution as obtained by design-expert

Solution	Input parameters			Predicted values of results		Desirability
	A	B	C	TS (MPa)	MH (Hv)	
1	5.62	49.14	1001.25	180.00	300.00	0.8920
2	5.56	49.22	1009.70	180.48	300.00	0.8861
3	5.84	49.22	992.55	179.02	291.50	0.8527

Table 7. Comparison between the predicted values and the experimental values

Recommended parameters			Tensile strength (MPa)			Micro-hardness (Hv)		
A	B	C	Exp.	Pred.	PE (%)	Exp.	Pred.	PE (%)
5.62	49.14	1001.25	178.36	180	0.91	312.5	300	4.17
5.56	49.22	1009.70	170.28	180.48	5.65	289	300	3.67
5.84	49.22	992.55	171.57	179.02	4.16	305	291.5	4.63

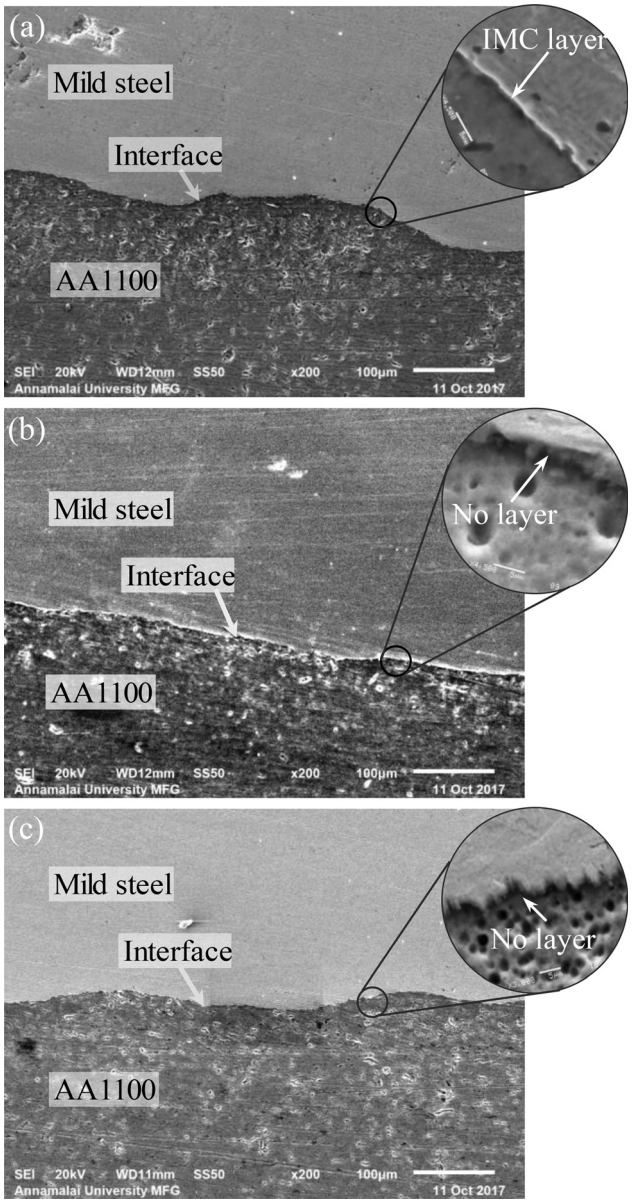

Figure 9. SEM images of the weld interface: (a) sample 7, (b) sample 11, (c) sample 8

value 49.22 MPa/s). This means that the thickness of the IMC layer formed at the weld interface is decreased with increasing forging pressure/time.

In order to analyze the microstructure at the welding interface and investigate the existing phases, an EDS analysis was performed on a selected sample containing an IMC layer (Sample 7). Figure 10 shows the EDS analysis results of three regions S, I, and A corresponding respectively to the side of the mild steel, the interface region and the aluminum side. It can be seen that both Fe and Al elements were detected along the interface between the aluminum and the steel base materials which illustrates the presence of an IMC layer of Fe and Al. The formation of this IMC layer at the weld interface of sample 7 may be the most probable reason for the weakness of its joint, whereas the disappearance of this layer increases the joint strength [31].

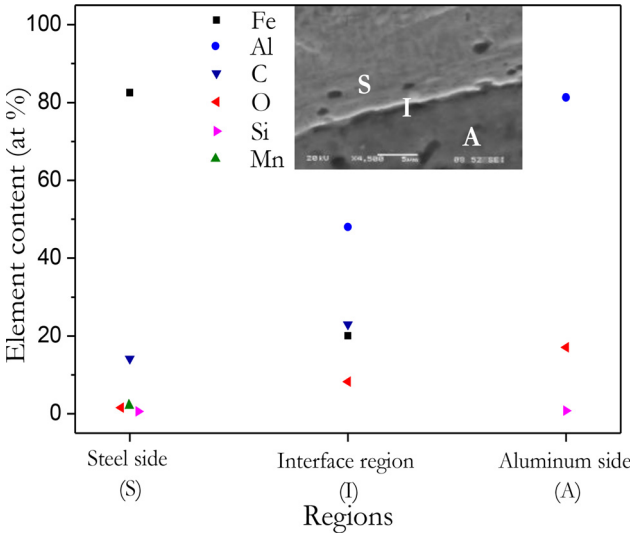

Figure 10. The EDS analysis results of sample (7)

4. CONCLUSIONS

Based on RSM – which is a collection of mathematical and statistical techniques used for designing the experiments – an empirical relationship was developed to predict the tensile strength and hardness of friction welded AA1100 aluminum alloy and mild steel joints. This study led to the following results:

1. The empirical relationships developed can be effectively employed to predict the tensile strength and the hardness of friction welded joints.
2. The RSM analysis shows that the maximum strength of joints could be attained under the maximum level of forging pressure/time, while the minimum level product a minimum hardness in the weld joints.
3. The SEM observations revealed the formation of an IMC layer at the interface of some welds, which represents the most probable cause to justify the weakening of these joints.

ACKNOWLEDGMENTS

The authors thank the Algerian Research Organism DGRSDT for its financial support. The authors are grateful to Dr V. Balasubramanian, Director of CEMAJOR (Centre for Materials Joining and Research) – Annamalai University – India, for extending the facilities of metal joining and material testing to carry out this work. The authors also acknowledge all CEMAJOR staff for their helpful assistance.

REFERENCES

[1] S. Fukumoto, H. Tsubakino, K. Okita, M. Aritoshi, and T. Tomita, "Amorphization by friction welding between 5052 aluminum alloy and 304 stainless steel." *Scripta Mater.*, vol. 42, pp. 807–812, 2000.

[2] L. Agudo, D. Eyidi, C. H. Schmaranzer, E. Arenholz, N. Jank, J. Bruckner, and A. R. Pyzalla, "Intermetallic Fe_xal_y-Phases in a steel/Al-alloy fusion weld." *J. Mater. Sci.*, vol. 42, pp. 4205–4214, 2007.

[3] S. Fukumoto, H. Tsubakino, K. Okita, M. Aritoshi, and T. Tomita, "Microstructure of friction weld interface of 1050 aluminium to austenitic stainless steel." *Mater. Sci. Technol.*, vol. 14, pp. 333–338, 1998.

[4] W. B. Lee, Y. M. Yeo, D. U. Kim, and S. B. Jung, "Effect of friction welding parameters on mechanical and metallurgical properties of aluminium alloy 5052–A 36 steel joint." *Mater. Sci. Technol.*, vol. 19, pp. 773–778, 2003.

[5] M. Sahin, "Joining of aluminium and copper materials with friction welding." *Int. J. Adv. Manuf. Technol.*, vol. 49, pp. 527–534, 2010.

[6] A. B. Dawood, S. I. Butt, G. Hussain, M. A. Siddiqui, A. Maqsood, and F. Zhang, "Thermal model of rotary friction welding for similar and dissimilar metals." *Metals*, vol. 7, pp. 1–14, 2017.

[7] B. S. Yilbas, A. Z. Sahin, A. Coban, and B. J. Abdul-Aleem, "Investigation into the properties of friction welded aluminum bars." *J. Mater. Process. Technol.*, vol. 54, pp. 76–81, 1995.

[8] S. Celik, A. D. Karaoglan, and I. Ersozlu, "An effective approach based on response surface methodology for predicting friction welding parameters." *High Temp. Mater. Process.*, vol. 35, pp. 235–241, 2015.

[9] S. T. Selvamani, K. Palanikumar, K. Umanath, and D. Jayaperumal, "Analysis of friction welding parameters on the mechanical metallurgical and chemical properties of AISI 1035 steel joints." *Mater. Des.*, vol. 65, pp. 652–666, 2015.

[10] N. Özdemir, "Investigation of the mechanical properties of friction–welded joints between AISI 304L and AISI 4340 steel as a function rotational speed." *Mater. Lett.*, vol. 59, pp. 2504–2509, 2005.

[11] W. Li, A. Vairis, M. Preuss, and T. Ma, "Linear and rotary friction welding review." *Int. Mater. Rev.*, vol. 61, pp. 71–100, 2016.

[12] A. Z. Sahin, B. S. Yilbas, and A. Z. Al-Garni, "Friction welding af Al–Al, Al–steel, and steel–steel samples." *J. Mater. Eng. Perform.*, vol. 5, pp. 89–99, 1996.

[13] S. Fukumoto, T. Inuki, H. Tsubakino, K. Okita, M. Aritoshi, and T. Tomita, "Evaluation of friction weld interface of aluminum to austenitic stainless steel joint." *Mater. Sci. Technol.*, vol. 13, pp. 679–686, 1997.

[14] S. Fukumoto, H. Tsubakino, K. Okita, M. Aritoshi, and T. Tomita, "Friction welding process of 5052 aluminum alloy to 304 stainless steel." *Mater. Sci. Technol.*, vol. 15, pp. 1080–1086, 1999.

[15] M. Kimura, K. Suzuki, M. Kusaka, and K. Kaizu, "Effect of friction welding condition on joining phenomena, tensile strength, and bend ductility of friction welded joint between pure aluminium and AISI 304 stainless steel." *J. Manuf. Process.*, vol. 26, pp. 178–187, 2017.

[16] M. Kimura, M. Kusaka, K. Kaizu, K. Nakata, and K. Nagatsuka, "Friction welding technique and joint properties of thin–walled pipe friction–welded joint between type 6063 aluminum alloy and AISI 304 austenitic stainless steel." *Int. J. Adv. Manuf. Technol.*, vol. 82, pp. 489–499, 2016.

[17] M. Sahin, "Joining of stainless–steel and aluminum materials by friction welding." *Int. J. Adv. Manuf. Technol.*, vol. 41, pp. 487–497, 2009.

[18] E. P. Alves, F. P. Neto, and C. Y. An, "Welding of AA1050 aluminum with AISI 304 stainless steel by rotary friction welding process." *J. Aero. Technol. Manag.*, vol. 2, pp. 301–306, 2010.

[19] S. D. Meshram and G. M. Reddy, "Friction welding of AA6061 to AISI 4340 using silver interlayer." *Defence Technol.*, vol. 11, pp. 292–298, 2015.

[20] L. Wan and Y. Huang, "Friction welding of AA6061 to AISI 316L steel: characteristic analysis and novel design equipment." *Int. J. Adv. Manuf. Technol.*, vol. 95, pp. 4117–4128, 2018.

[21] R. Paventhan, R. Lakshminarayanan, and V. Balasubramanian, "Prediction and optimization of friction welding parameters for joining aluminum alloy and stainless steel." *Trans. Nonferrous Metals Soc. China*, vol. 21, pp. 1480–1485, 2011.

[22] A. Pachal and A. Bagesar, "Taguchi optimization of process parameters in friction welding of 6061 aluminum alloy and 304 steel: a review." *Int. J. Emerg. Technol. Adv. Eng.*, vol. 3, pp. 229–233, 2013.

[23] N. Mathiazhagan, T. S. Kumar, and M. Chandrasekar, "Optimization of friction welding parameters for AISI 304/AA6061 dissimilar metal joint using RSM/ANFIS." *Asian J. Res. Soc. Sci. Humanit.*, vol. 6, pp. 2089–2105, 2016.

[24] C. H. Lauro, R. B. D. Pereira, L.C. Brandao, L.C. Brandao, and J. P. Davim, "Design of experiments–statistical and artificial intelligence analysis for the improvement of machining processes: a review," in *Design of Experiments in Production Engineering*, Cham: Springer, pp. 89–107, 2016.

[25] R. H. Myers, D. C. Montgomery, and C. M. Anderson-Cook, *Response Surface Methodology – Process and Product Optimization using Designed Experiment*, 4th ed. New Jersey: John Wiley & Sons, 2016.

[26] I. Dinaharan, N. Murugan, and A. Thangarasu, "Development of empirical relationships for prediction of mechanical and wear properties of AA6082 aluminum matrix composites produced using friction stir processing." *Eng. Sci. Technol. Int. J.*, vol. 19, pp. 1132–1144, 2016.

[27] E. Raouache, N. Logzit, Z. Driss, and F. Khalfallah, "Optimization by RSM of reinforced concrete beam process parameters." *Am. J. Mech. Eng.*, vol. 6, pp. 66–74, 2018.

[28] S. Rajakumar and V. Balasubramanian, "Microstructure and mechanical properties of electrical resistance spot welded interstitial free steel joints." *J. Adv. Micros. Res.*, vol. 10, pp. 146–154, 2015.

[29] P. Sammaiah, A. Suresh, and G. R. N. Tagore, "Mechanical properties of friction welded 6063 aluminum alloy and austenitic stainless steel." *J. Mater. Sci.*, vol. 45, pp. 5512–5521, 2010.

[30] A. K. Lakshiminarayanan and V. Balasubramanian, "Comparison of RSM with ANN in predicting tensile strength of friction stir welded AA7039 aluminum alloy joints." *Trans. Nonferrous Metals Soc. China*, vol. 19, pp. 9–18, 2009.

[31] A. Ambroziak, M. Korzeniowski, P. Kustron, M. Winnicki, P. Sokolowski, and E. Harapinska, "Friction welding of aluminium and aluminium alloys with steel." *Adv. Mater. Sci. Eng.*, vol. 2014, pp. 1–15, 2014.